

## FEATURE ARTICLE

# Alterations in Anatomical Covariance in the Prematurely Born

Dustin Scheinost<sup>1,7</sup>, Soo Hyun Kwon<sup>2</sup>, Cheryl Lacadie<sup>1</sup>, Betty R. Vohr<sup>6</sup>, Karen C. Schneider<sup>2</sup>, Xenophon Papademetris<sup>1,3</sup>, R. Todd Constable<sup>1,4</sup> and Laura R. Ment<sup>2,5</sup>

<sup>1</sup>Department of Diagnostic Radiology, <sup>2</sup>Department of Pediatrics, <sup>3</sup>Department of Biomedical Engineering, <sup>4</sup>Department of Neurosurgery, <sup>5</sup>Department of Neurology, Yale University School of Medicine, New Haven, CT, USA, <sup>6</sup>Department of Pediatrics, Warren Alpert Brown Medical School, Providence, RI, USA and <sup>7</sup>Magnetic Resonance Research Center, New Haven, CT 06520-8043, USA

Address correspondence to Dustin Scheinost, PhD, Magnetic Resonance Research Center, 300 Cedar St, PO Box 208043, New Haven, CT 06520-8043, USA. Email: dustin.scheinost@yale.edu

R. Todd Constable and Laura R. Ment contributed equally to this work.

## Abstract

Preterm (PT) birth results in long-term alterations in functional and structural connectivity, but the related changes in anatomical covariance are just beginning to be explored. To test the hypothesis that PT birth alters patterns of anatomical covariance, we investigated brain volumes of 25 PTs and 22 terms at young adulthood using magnetic resonance imaging. Using regional volumetrics, seed-based analyses, and whole brain graphs, we show that PT birth is associated with reduced volume in bilateral temporal and inferior frontal lobes, left caudate, left fusiform, and posterior cingulate for prematurely born subjects at young adulthood. Seed-based analyses demonstrate altered patterns of anatomical covariance for PTs compared with terms. PTs exhibit reduced covariance with R Brodmann area (BA) 47, Broca's area, and L BA 21, Wernicke's area, and white matter volume in the left prefrontal lobe, but increased covariance with R BA 47 and left cerebellum. Graph theory analyses demonstrate that measures of network complexity are significantly less robust in PTs compared with term controls. Volumes in regions showing group differences are significantly correlated with phonological awareness, the fundamental basis for reading acquisition, for the PTs. These data suggest both long-lasting and clinically significant alterations in the covariance in the PTs at young adulthood.

**Key words:** anatomical covariance, connectivity, structural covariance, preterm, young adulthood

## Introduction

Preterm (PT) birth represents a global health problem (Beck et al. 2010) with PT infants at high risk of brain injury and future cognitive impairment (Saigal and Doyle 2008; Hack 2009). Language delays, fine motor difficulties, and executive function problems are common in PT toddlers (Foster-Cohen et al. 2010) and related academic difficulties persist through childhood into young adulthood (Hille et al. 2007; Pritchard et al. 2014; Vohr et al. 2014).

Alterations in the development of brain structure and function have been postulated as predictors of these developmental outcomes (Kwon et al. 2014). Using magnetic resonance imaging (MRI), the structural consequences of PT birth on the developing brain are well documented. Smaller cortical and subcortical volumes are consistently observed in PT infants (Inder et al. 1999; Ball et al. 2012), children (Peterson et al. 2000), and adolescents (Nosarti et al. 2008). Similarly, regional differences in white

matter volumes are observed across the same time interval (Peterson et al. 2003; Giménez et al. 2006). While emerging research suggests that structural alterations attributable to PT birth are long-lasting (Bjuland et al. 2014; Nosarti et al. 2014; Aanes et al. 2015), investigations of young adults born PT have been relatively less explored.

Traditionally, such structural analyses have concentrated on focal regional differences (Bjuland et al. 2014; Aanes et al. 2015). However, morphological features of different brain regions are not independent of those of other areas, and the brain shows a high level of coordination between different structures (Mechelli et al. 2005; Raz et al. 2005; Lerch et al. 2006). This coordination, or covariance, of morphological features is often referred to as anatomical covariance (Mechelli et al. 2005; Evans 2013) and appears to be a key marker of typical development present in early childhood (Zielinski et al. 2010, 2012; Raznahan et al. 2011; Alexander-Bloch, Raznahan, et al. 2013; Zielinski et al. 2014). Using regions of interest (ROIs), or “seeds,” patterns of anatomical covariance have been linked to developmental disorders such as schizophrenia (Mitelman et al. 2005) and autism (Zielinski et al. 2012). Similarly, seed-based patterns of anatomical covariance in PT subjects at age 14–15 years suggest that changes in language regions may alter the development of other structurally related regions (Nosarti et al. 2008, 2011).

In addition to seed-based approaches, network-level approaches for anatomical covariance have recently been developed (He et al. 2008; Bernhardt et al. 2011; Chen et al. 2011; Alexander-Bloch, Raznahan, et al. 2013). These approaches interrogate the covariance patterns of every pair-wise combination of brain regions, forming a network or graph. The topography of these graphs can then be summarized using graph theory measures. As covariance patterns are not limited to only a small number of seed regions, a more complete picture of anatomical covariance and their alterations in PT birth can be observed.

To test the hypothesis that PT birth alters patterns of brain morphometry at regional, seed, and network levels, we investigated brain volumes of 25 prematurely born participants and 22 term controls at young adulthood using anatomical MRIs. Tensor-based morphometry (TBM; Staib et al. 2006) was used to calculate voxel-wise estimates of volume, which were used for comparisons of regional volume and seed-based patterns of anatomical covariance. Finally, graphs of anatomical covariance were created, and graph theory metrics of segregation and integration were compared between study groups, providing for the first time a whole brain measure of anatomical covariance in PT subjects at young adulthood.

## Methods

This study was performed at the Yale University School of Medicine, New Haven, CT, and Warren Alpert Brown Medical School, Providence, RI. The protocols were reviewed and approved by institutional review boards at each location. Written consent was obtained from all study participants. All scans were obtained and analyzed at the Yale University School of Medicine.

### Participants

The participants consisted of a cohort of 25 prematurely born young adults with no evidence of intraventricular hemorrhage (IVH), periventricular leukomalacia, and/or low-pressure ventriculomegaly. Excluding these common brain injuries allows for the investigation of the primary sequelae of premature birth, not secondary effects related to brain injuries. All PT participants

**Table 1** Demographic and cognitive data for the study participants

	Preterm (N = 25)	Term (N = 22)	P-value
Male, n (%)	13 (52)	10 (45)	0.77
Age at scan, years ± SD	20 ± 0.96	19.74 ± 1.09	0.38
Left-handed, n (%)	3 (12)	1 (4.5)	0.61
Non-white, n (%)	7 (28)	6 (27)	0.99
Maternal education, years ± SD	13.63 ± 2.45	14.95 ± 2.77	0.09
Age at assessment, years ± SD	16.1 ± 0.09	16.26 ± 0.29	0.01
WISC-III			
FSIQ, mean ± SD	91.75 ± 11.96	103.14 ± 19.23	0.03
PIQ, mean ± SD	93.08 ± 12.73	106.62 ± 20.04	0.01
VIQ, mean ± SD	91.96 ± 11.67	99.67 ± 17.58	0.10
Verbal comprehension index	92.46 ± 11.48	99.38 ± 11.48	0.12
PPVT			
PPVT, mean ± SD	99.67 ± 18.76	102.55 ± 23.49	0.65
CTOPP			
Rapid naming, mean ± SD	103 ± 20.6	97.82 ± 13.2	0.31
Phonological awareness, mean ± SD	80.36 ± 11.95	90.04 ± 10.72	0.007

**Table 2** Demographic and cognitive data for the study participants

	Preterm
Birth weight, g ± SD (range)	962.7 ± 170.1 (660–1200)
Gestational age, weeks ± SD (range)	28.1 ± 1.78 (25–31)
BPD, n (%)	6 (24)
Necrotizing enterocolitis, n (%)	0 (0)
Retinopathy of prematurity, n (%)	9 (36)
5 min APGAR score, median (range)	7 (4–9)

consisted of young adults who were enrolled in the follow-up MRI component of the Multicenter Randomized Indomethacin IVH Prevention Trial at the Yale University School of Medicine and Brown University (Ment et al. 1994). Only those PT young adults who lived within 200 miles of the Yale MRI research facility were eligible for this protocol. Participants were between 18 and 22 years old, with a mean age of 20 ± 0.96 years. Demographic data are provided in Table 1.

Neonatal characteristics of the PT participants are provided in Table 2. The PT participants weighed between 660 and 1200 g at birth (mean birth weight of 962.7 ± 170.1 g) and were born between 25 and 31 weeks of gestation (mean gestational age of 28.1 ± 1.8 weeks).

Twenty-two term control young adults were recruited from the local communities of the study children. They were group-matched to the PT young adults for age, sex, handedness, and minority status as summarized in Table 1.

While PT participants were screened and excluded based on a previous history of structural brain abnormalities, scans for all PT and term participants were additionally read by an attending neuroradiologist blinded for group and neonatal hospital course. All scans were free of structural abnormalities.

### Neurodevelopmental Assessments

The assessments of neonatal health status and neurologic outcome have been outlined in prior work (Peterson et al. 2000). Full cognitive assessment for both term and PT participants was performed approximately 4 years before imaging when

participants were 16 years old. Blinded assessment of intelligence was performed using the Wechsler Intelligence Scale for Children-III (WISC-III). Participants also received the Peabody Picture Vocabulary Test-Revised (PPVT-R) and composite scores of the Comprehensive Test of Phonological Processing (CTOPP), including Rapid Naming and Phonological Awareness. For a subset of the participants (18 PTs and 8 terms), a brief cognitive assessment, including the CTOPP and the PPVT, was performed at age 20 years on the same day as the imaging.

### Imaging Parameters

Participants were scanned in a Siemens 3-T Tim Trio scanner. After a first localizing scan, a high-resolution 3D volume was collected using a magnetization-prepared rapid gradient-echo sequence (176 contiguous sagittal slices, slice thickness 1 mm, matrix size 192 × 192, field of view = 256 mm, time repetition = 2530 ms, time echo = 2.77 ms, and flip angle = 7°).

### Tensor-Based Morphometry

First, images were skull-stripped using FSL BET (Smith 2002) and any remaining nonbrain tissue was manually removed. All further analysis was performed using BioImage Suite (Joshi et al. 2011) unless otherwise specified. Images were aligned to the MNI space using a 12-parameter affine registration by maximizing the normalized mutual information (Studholme et al. 1999) between individual scans and the MNI template brain. These aligned images were averaged together to form the initial template using a nonlinear registration.

For TBM analysis, images were nonlinearly registered to an evolving group-average template in an iterative fashion. This algorithm iterates between estimating a local transformation to align individual brains to a group-average template and creating a new group-average template based on the previous transformations. The local transformation was modeled using a free-form deformation parameterized by cubic B-splines (Rueckert et al. 1999; Papademetris et al. 2004). This transformation deforms an object by manipulating an underlying mesh of control points. The deformation for voxels in between control points was interpolated using B-splines to form a continuous deformation field. Positions of control points were optimized using conjugate gradient descent to maximize the normalized mutual information between the template and individual brains. After each iteration, the quality of the local transformation was improved by increasing the number of control points and decreasing the spacing between control points to capture a more precise alignment. A total of 5 iterations were performed with decreasing control point spacings of 15, 10, 5, 2.5, and 1.25 mm. To help prevent local minimums during optimization, a multiresolution approach was used and 3 resolution levels were used at each iteration.

The determinant of the Jacobian of the deformation field was used to quantify local volume differences between the registered images and the template (Staub et al. 2006; Hua et al. 2008). This metric provides an estimate of voxel-wise volume changes for all transformed images with respect to the group-average template and was used for further analysis.

### Seed-Based Anatomical Covariance

Based on regions of significant volume differences, seed regions were chosen for standard anatomical covariance analysis. The volumes of these seed regions, calculated as the average

determinant of the Jacobian in the seed, were extracted and used as covariates in linear models (described below).

### Graph Theory Analysis of Anatomical Covariance

Graphs of anatomical covariance, consisting of 82 cortical and subcortical regions, were created separately for the term and PT groups using the Yale Brodmann atlas. For each participant, the volume (average determinant of the Jacobian) for each region was calculated. Next, across subject correlation of each region's volume with every other region's volume was computed, resulting in an 82 × 82 correlation matrix for each group. Any element in these 2 correlation matrices represents the correlation of the volume for any 2 Brodmann areas (BAs) across either the term or PT participants. Weighted and binary graphs were created. For weighted graphs, the edge weights between nodes were assumed to be the correlation coefficients between brain regions. To create binary graphs, the correlation matrices were thresholded using a range of density thresholds with any edge greater than the threshold set to "1" and any edge less than the threshold set to "0." Density thresholds ranged from 5% (the minimum threshold where all graphs were fully connected) to 70% in 5% increments. Using multiple definitions of the graph model ensures that group differences are not dependent on arbitrary factors such as thresholds (Scheinost et al. 2012; Garrison et al. 2015).

For all graphs, 2 measures were chosen to explore the topography of the anatomical covariance graphs: Clustering coefficient and global efficiency. For weighted graphs, average strength was also explored. Clustering coefficient measures are the extent to which nodes in a graph tend to cluster together and provide a measure of local information transfer. Global efficiency is a measure of information transfer over all the nodes. Complex networks, such as those in the brain, are associated with high clustering coefficients and global efficiency, indicating a greater level of robustness and efficient information transfer (Bullmore and Sporns 2009). Strength is the sum of the weights for any node in a graph. Further information about these metrics can be found elsewhere (Rubinov and Sporns 2010). Graph theory analysis was performed using the Brain Connectivity Toolbox (<https://sites.google.com/site/bctnet>).

### Exploratory Analyses of Language and Neonatal Risk Factors

Based on regions of significant TBM differences, volumes from these regions were correlated with language measures at age 16 years (Table 1) and neonatal risk factors (Table 2). Standard scores were used for all language measures.

### Statistics

TBM and seed anatomical covariance data were analyzed with voxel-wise general linear modeling. Age at scan and sex were included as covariates. For models of anatomical covariance, seed volumes and a group-by-volume interaction were added as covariates of interest. Significant group-by-volume interactions describe brain regions that show group differences in the correlation between their volume and the seed region's volume. Multiple comparisons were corrected for using Monte Carlo simulation (AFNI AlphaSim). Input smoothness for these simulations was estimated from the residuals of the GLMs. Volume results are shown at  $P < 0.005$  corrected with an initial  $P$  threshold of  $P < 0.005$  and anatomical covariance results are shown at  $P < 0.05$  corrected with an initial  $P$  threshold of  $P < 0.05$ . The lower  $P$ -value for anatomical covariance results is based on the



assumption that seed-based analysis would produce more widespread patterns similar to patterns of resting-state functional networks. Results are overlaid onto the final group-average template. Partial correlations controlling for sex and age at scan were employed to examine the relationships between volume and cognitive outcome measures. Permutation testing with 10 000 permutations was used to compare the graph theory measures between each group.  $P$ -values of  $<0.05$  were considered significant.

Demographic and cognitive data were analyzed either using standard  $\chi^2$  statistics or using Fisher's exact test for categorical data. Continuous-valued data were analyzed either using  $t$ -tests or Mann-Whitney  $U$ -test when a normal distribution could not be assumed to compare groups. For the purposes of this report,  $P$ -values of  $<0.05$  were considered significant. For exploratory analyses, presented  $P$ -values are left uncorrected for multiple comparisons to present preliminary findings and to aid possible future studies. All analyses were performed using MATLAB 2011b (MathWorks, Natick, MA, USA).

## Results

### Participants and Neurodevelopmental Assessment

As provided in Table 1, there were no significant differences between the PT and term groups in gender, age at scan, handedness, minority status, or maternal education. Using the assessment data at age 16 years, term participants were on average 2 months

older at the age of neuropsychological testing. There were no significant differences between the study groups for verbal IQ (VIQ), the Rapid Naming composite score of the CTOPP, or the PPVT-R. PT participants scored significantly ( $P < 0.05$ ) lower than term participants on performance IQ (PIQ), full scale IQ (FSIQ), and the Phonological Awareness composite score of the CTOPP. For participants with assessment data at both age 16 and 20 years, the correlations between the data at both time points were significant ( $r > 0.80$ ,  $P < 0.0001$ ). Full analysis of the assessment data of both times is presented in [Supplementary Material and Table 1](#).

### Tensor-Based Morphometry

For PT participants compared with term controls, the TBM analysis revealed significantly ( $P < 0.005$ , corrected) reduced volume in bilateral temporal lobes (BA 21), bilateral inferior frontal lobes (BA 47), posterior cingulate cortex (PCC)/corpus callosum, right caudate, and motor cortex as shown in Figure 1. In addition, since there was a significant difference in IQ for the study groups, we independently covaried the results by FSIQ, PIQ, and VIQ, and found no change in the results in any of these analyses.

### Seed-Based Anatomical Covariance

The 7 regions described above were used as seeds for traditional anatomical covariance analyses. For PT participants compared with term controls, the volumes of the R BA 47 (Fig. 2A), L BA 21

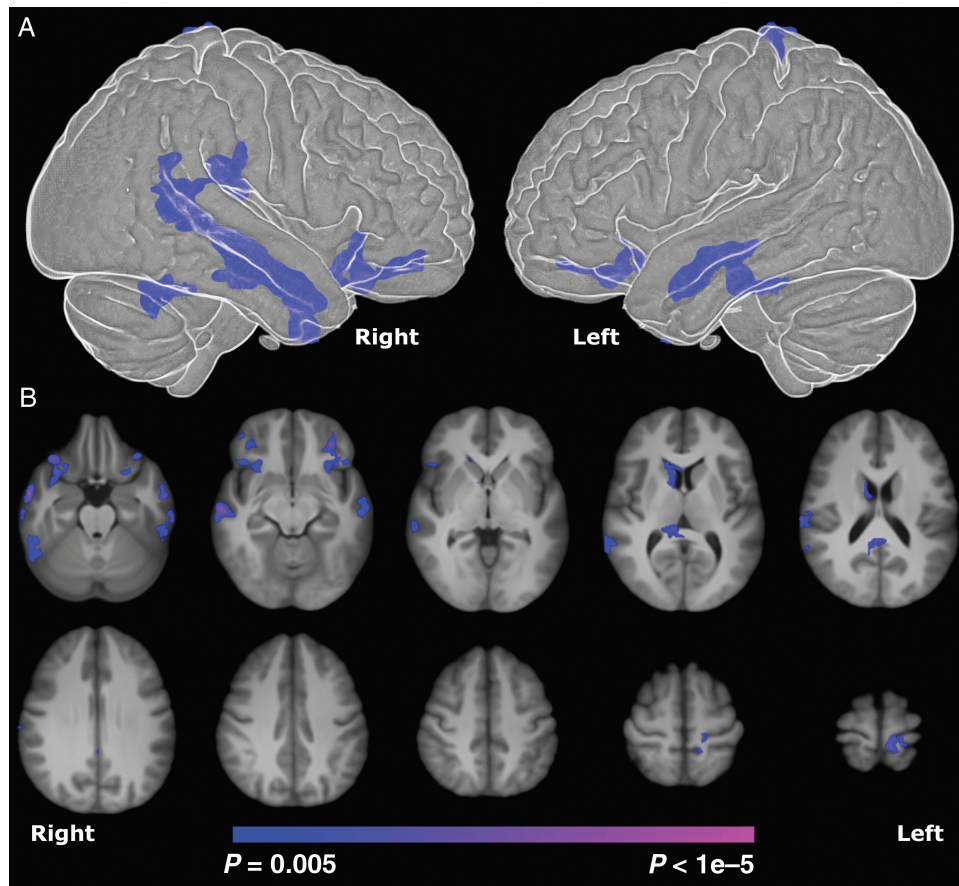


**Figure 1.** Comparison of regional volume difference in PT and term young adults derived from TBM. (A) Surface rendering of TBM results showing significantly reduced volume in bilateral temporal and inferior frontal lobes for PT young adults. The differences were mainly localized to bilateral BA 21 and 47. (B) Axial views of TBM results showing significantly reduced ( $P < 0.005$  corrected) subcortical volume in the right caudate and white matter volume near the PCC for PT young adults. Differences are shown overlaid on the final group-average template. Surface rendering was created using [Biolmage Suite \(Joshi et al. 2011\)](#).

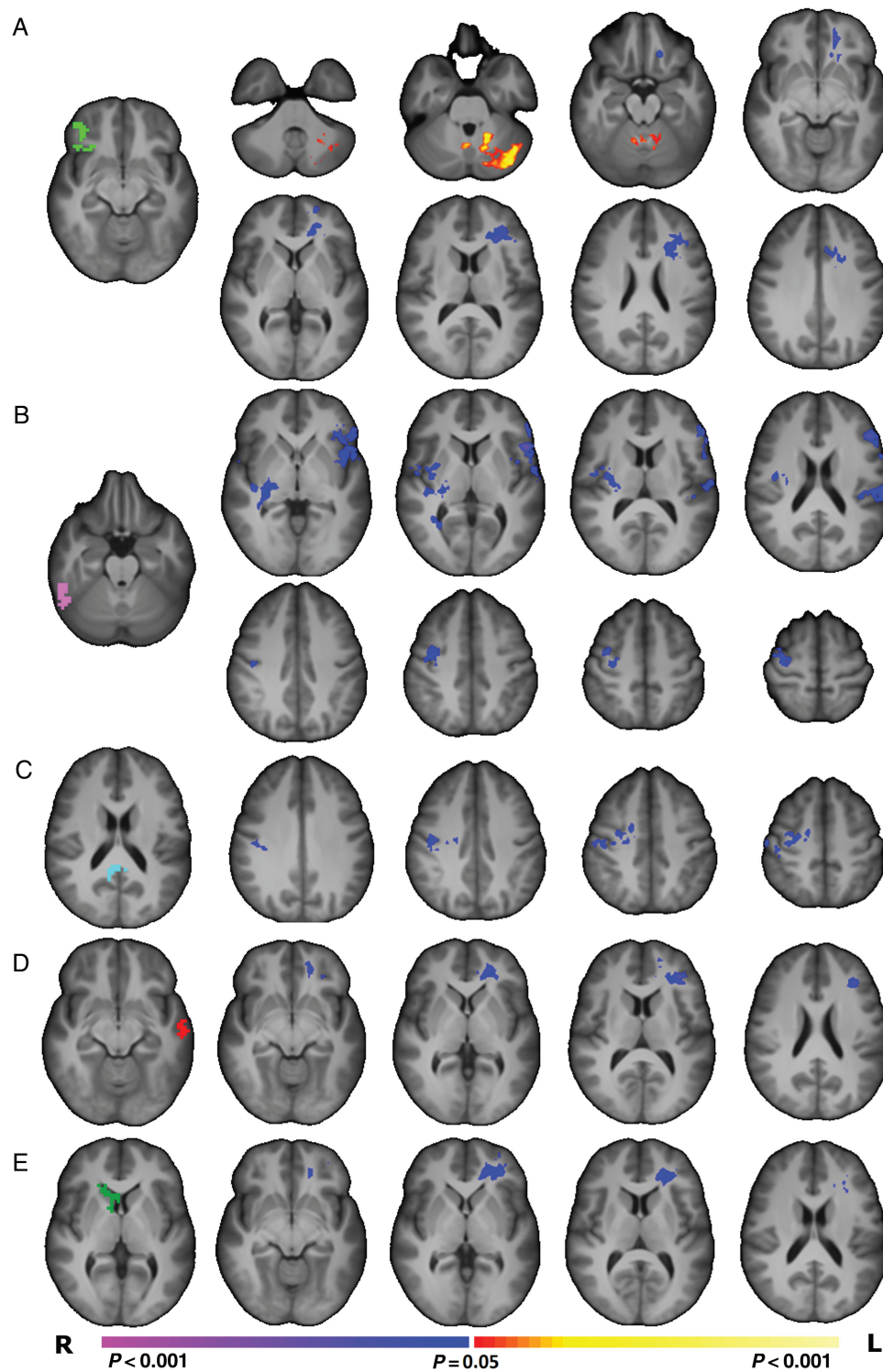


**Figure 2.** Comparison of seed anatomical covariance patterns between PT and term young adults. (A) PT participants showed significantly ( $P < 0.05$ , corrected) reduced correlation between the volume of the R BA 47 seed region (shown in green) and the volume of the white matter in the left prefrontal lobe. Additionally, volume of the R BA 47 seed region showed a significantly ( $P < 0.05$ , corrected) greater correlation with left cerebellar volume for PT participants compared with term participants. (B) PT participants showed significantly ( $P < 0.05$ , corrected) reduced correlation between the volume of the R fusiform seed region (shown in pink) and the volume in the left interior frontal lobe, right temporal-parietal junction, and right motor regions. (C) PT participants showed significantly ( $P < 0.05$ , corrected) reduced correlation between the volume of the PCC seed region (shown in teal) and the volume of right motor regions. (D) PT participants showed significantly ( $P < 0.05$ , corrected) reduced correlation between the volume of the L BA 21 seed region (shown in red) and the volume of the white matter in the left prefrontal lobe. (E) PT participants showed significantly ( $P < 0.05$ , corrected) reduced correlation between the volume of the R caudate seed region (shown in green) and the volume of the white matter in the left prefrontal lobe.

(Fig. 2C), and caudate seeds (Fig. 2E) were significantly less correlated ( $P < 0.05$ , corrected) with white matter volumes in the left prefrontal lobe ( $P < 0.05$ , corrected). Additionally, the volume of the R BA 47 seed was significantly more correlated ( $P < 0.05$ , corrected) with left cerebellar volume in inferior and superior semilunar, simple, biventer, and quadrangular lobules for PT participants (Fig. 2A). For PT participants compared with term controls, the volume of the fusiform seed was significantly less correlated ( $P < 0.05$ , corrected) with regions of the left inferior frontal gyrus, bilateral gray, and white matter near the temporal–parietal junction and right motor cortex (Fig. 2B). Similarly, the PCC was significantly less correlated ( $P < 0.05$ , corrected) with regions of the right motor cortex (Fig. 2C). There were no significant differences in anatomical covariance detected with the R BA 21, L BA 47, or motor seeds.

### Graph Theory Analysis of Anatomical Covariance

Using 82 regions to create group-level correlation matrices, PT and term participants showed a high level of coordination between the volumes of each region. However, PT participants showed significantly reduced average pair-wise correlations between regions (i.e., “strength”) compared with term subjects ( $P < 0.05$ , corrected, permutation test; Fig. 3). In addition, PT participants showed a reduced clustering coefficient averaged across all nodes in the graph compared with the term controls for the weighted graph (PTs:  $0.365 \pm 0.06$ ; terms:  $0.467 \pm 0.07$ ,  $P < 0.05$ ,

corrected, permutation test) and at several density thresholds for the binary graph ( $P < 0.05$ , corrected, permutation test; Fig. 3). No differences in global efficiency between the groups were observed for the weighted (PTs:  $0.35 \pm 0.10$ ; terms:  $0.40 \pm 0.10$ ) or binary graphs (Fig. 3).

After correcting for multiple comparisons, exploratory nodal analysis of strength and clustering coefficient for the weighted graphs revealed no significant nodal differences between groups. Nodes with the largest between-group differences were generally located within somatomotor and somatosensory regions (not shown).

### Exploratory Correlation Analyses

Since BA 21 and BA 47 are part of a complex language network, we explored the hypothesis that the volume in these regions would be significantly correlated with language assessment measures for the PT participants but not for term controls. For the PT subjects, the Phonological Awareness composite score of the CTOPP was significantly correlated ( $P < 0.05$ , uncorrected), while controlling for sex and age at scan, with volumes in both R and L BA 47 regions and L BA 21. Additionally, FSIQ and PIQ were significantly correlated ( $P < 0.05$ , uncorrected), while controlling for sex and age at scan, with volume in R BA 21.

For the term participants, there were no significant correlations between volume in these regions and the Phonological Awareness composite score. In contrast, FSIQ was significantly

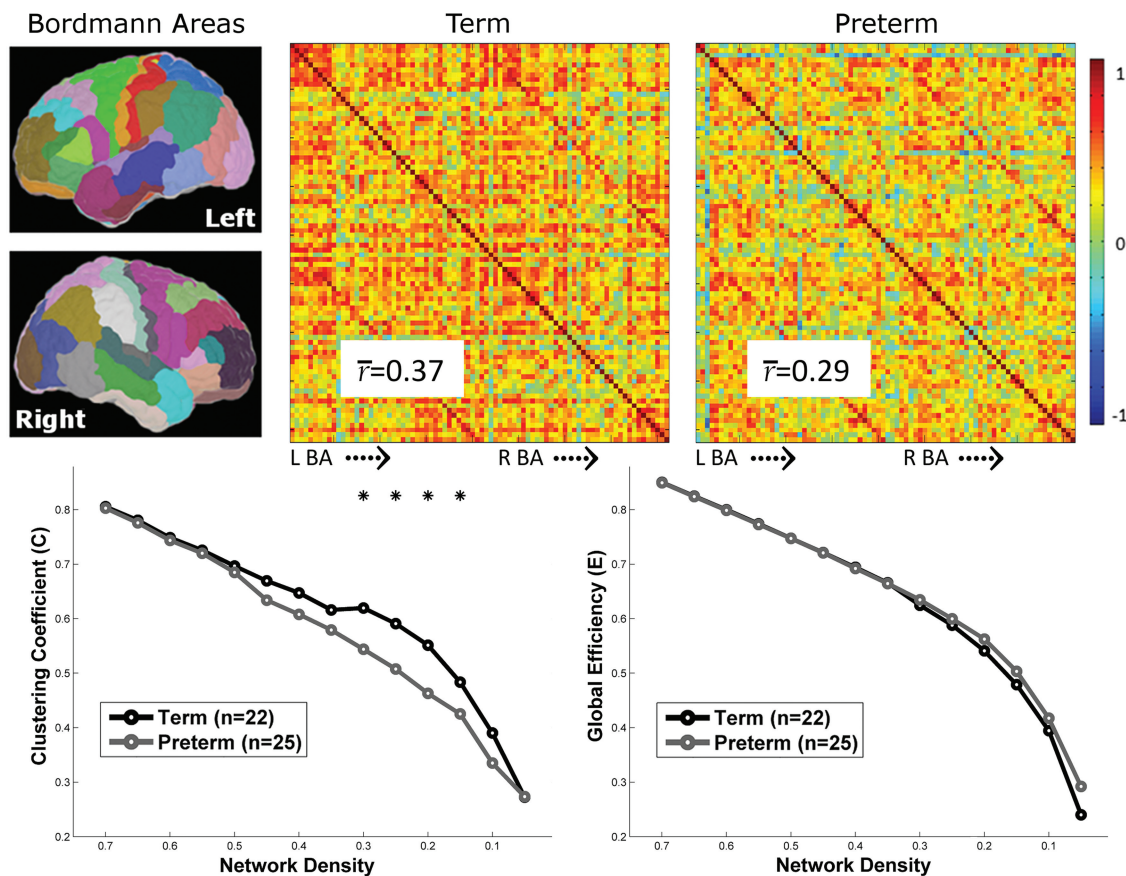


**Figure 3.** Comparison of graphs of anatomical covariance between PT and term participants. (Top) Eighty-two anatomical regions based on the Yale Brodmann atlas were used to create group-level correlation matrices of anatomical covariance. Both groups showed a high level of coordination between the volumes of each region; yet, PT participants showed significantly reduced average pair-wise correlation between regions ( $P < 0.05$ , permutation test) compared with term participants. (Bottom) Binary graphs at several density thresholds were created from these correlation matrices. Clustering coefficient, but not global efficiency averaged across all nodes in the graph, was significantly reduced in PT participants. Asterisks indicate threshold which group differences were observed at  $P < 0.05$  using permutation testing.



correlated ( $P < 0.05$ , uncorrected), while controlling for sex and age at scan, with volume in R BA 21. Neither study group showed significant correlations between volumes in these regions and the PPVT, VIQ, or the Rapid Naming composite score. Additional analysis with the assessment of data at 20 years of age is presented in [Supplementary Material](#).

Exploratory analyses testing the hypotheses that gestational age, gender, APGAR scores, bronchopulmonary dysplasia (BPD), and/or the presence of a patent ductus arteriosus at postnatal age 5 days would be associated with morphometric data yielded no significant results.

## Discussion

Twenty years after their birth, the PT young adults in this study demonstrate significant alterations in the developing brain. Using regional volumes and seed anatomical covariance strategies, we show that PT birth is associated with altered patterns of covariance and morphometry in the bilateral temporal and inferior frontal lobes, and caudate in PT subjects compared with term controls; these findings are significantly correlated with a critical measure of language, phonological processing, in this vulnerable population. Measures of network complexity and strength were significantly less in PT participants, suggesting both widespread and long-lasting alterations in cortical development in the prematurely born.

Anatomical covariance of developing brain and the impact of PT birth are just beginning to be explored. White matter and gray matter differences in PT adolescents compared with term controls at 14–15 years of age have been shown to be highly correlated with each other, suggesting that these altered structures are not independent of each other ([Nosarti et al. 2008](#)). Additionally, in a follow-up study, seed-based analyses of anatomical covariance suggested differential (both increased and decreased) covariance between frontal and cingulate gyri, caudate nucleus and cerebellum, as well as several other cortical and subcortical regions ([Nosarti et al. 2011](#)). Finally, significant associations between white matter injury and abnormalities in deep brain structures have been reported ([Boardman et al. 2006](#)), highlighting the influence that abnormalities in one brain area may exert over others.

The critical period for covariance has been postulated to occur in early childhood ([Zielinski et al. 2010, 2012, 2014](#); [Alexander-Bloch, Giedd, et al. 2013](#)), but recent data suggest that earlier events may alter this genetically determined phase of development. A rapid development of volume and connectivity occurs during the late second and third trimesters of gestation. During this period, total brain volume triples ([Volpe 2009](#)), white matter topology forms ([Ball et al. 2014](#)), and functional networks emerge ([Thomason et al. 2013, 2014](#)). When compared with term controls at term equivalent age, PT neonates show significant reduction in structural and functional network complexity and capacity, and hallmark brain topologies, such as rich club organization, have reported significant disruptions in both cortical–subcortical connectivity and short-distance cortico-cortical white matter connections ([Ball et al. 2014](#); [Scheinost et al. 2015a](#)). Similarly, ROI-based covariance analyses of functional connectivity demonstrated that both resting-state network complexity and magnitude are reduced in PT neonates ([Smyser et al. 2014](#)). Anatomical covariance may recapitulate, or be altered by, these white matter and functional networks in PT subjects at young adulthood ([Alexander-Bloch, Raznahan, et al. 2013](#)).

Anatomical covariance has been attributed to genetics, mutual trophic influences, and/or epigenetic events secondary to

environmental exposures of common experience-related plasticity ([Evans 2013](#)). The alterations in covariance we report may be secondary to the aberrant neurogenesis and synaptic maturation reported to occur in the prematurely born ([Komitova et al. 2013](#); [Back and Miller 2014](#)). Alternatively, early alterations in functional and structural networks ([Ball et al. 2014](#); [Scheinost et al. 2015a](#)) may disrupt later genetically programmed events, such as the coordinated growth of different brain regions. Furthermore, the impact of not only antenatal exposures, but also gestational age and early intervention strategies, on anatomical covariance remains largely unexplored. Additional analyses of these factors in larger cohorts may help identify both critical time points in the emergence of anatomical covariance in PTs and the factors that perturb them.

We used multiple complimentary approaches at regional, seed, and network levels to investigate alterations of morphological features in PT young adults. Regional analysis using TBM revealed several focal areas of reduced volume, in line with previous studies of PT young adults ([Nosarti et al. 2014](#)). However, given the large amount of coordination between different regions in the brain ([Alexander-Bloch, Giedd, et al. 2013](#)), it is not surprising that focal differences in brain volume could impact remote regions. These remote effects are not detectable using traditional TBM (or similar methods such as voxel-based or deformation-based morphometry), but are detectable with seed-based analyses. Using seed-based analysis, overlapping clusters in the right motor cortex and left prefrontal white matter were observed to demonstrate reduced covariance for several of the seeds, suggesting a possible network of altered morphological features. One weakness of the seed-based analyses is that differences in covariance can only be observed with reference to the chosen seed. To observe potential differences in nonhypothesized regions, data-driven approaches using whole brain graphs of anatomical covariance that test all pair-wise covariance patterns are needed. Significant between-group differences in strength and clustering coefficient provide further evidence that morphological features are altered at a network level without needing to examine “a priori” seeds. Taken together, these complimentary approaches suggest that alterations in morphological features in the PT brain are not only focal to specific brain regions, but also widespread, affecting global brain organization.

The graph theory analysis revealed that average strength and clustering coefficient, but not global efficiency, were significantly reduced in PT young adults. Reduced strength suggests a disruption in the “hubs” of the graph. Hubs are high strength nodes that allow a graph to form tight clusters of nodes (i.e. large clustering coefficient) while still permitting for efficient travel between these clusters (i.e. large global efficiency). As global efficiency was not reduced, individual nodes likely bypass these hubs and form their own connections between clusters. Likewise, the increased connections between all nodes in the graph would reduce the average clustering coefficient of a graph. Graphs with high cluster coefficient and high global efficiency are advantageous as they support specialized and integrated information processing ([Bassett and Bullmore 2006](#)). However, further work is needed to relate alterations in graph models of anatomical covariance to neurocognitive deficits in young adults born PT.

Many of our results were localized to regions involved in language processing and our exploratory correlation analysis suggested a relationship with these differences and phonological awareness. Phonological awareness, the ability to deconstruct a word into phonemes and manipulate them within a word, is the basis of reading acquisition ([Friederici 2009](#); [Saygin et al.](#)

2013), and was significantly lower in our PT sample. Increased volume in these regions was positively correlated with phonological awareness, suggesting that preserved volumes were associated with typically developing language. Regional volumes of differences were more pronounced in the right hemisphere; this may be related to observed reliance on alternative right hemisphere language regions in PT adolescents (Myers et al. 2010; Scheinost et al. 2015b; Wilke et al. 2014). Consistent with our previous report of increased functional connectivity between R inferior frontal gyrus and L cerebellum in PT subjects at age 20 years (Constable et al. 2013), PT participants in this study showed increased correlation between the volume of the right BA 47 seed and left cerebellum, a putative alternative language pathway.

The strengths of this study include innovative imaging strategies, prospective collection of subject data, and well-studied cohorts of both PT subjects and term controls at young adulthood. Covariance is developmentally regulated, and we report the first study of anatomical covariance of whole brain graphs in PT subjects and term controls at young adulthood. As PT subjects with brain injuries were excluded from our analyses, this permits for the important investigation of the impact of PT birth alone—not injury—on developing brain. The weaknesses include small sample size, lack of neonatal MRI studies for the PT subjects, and failure to demonstrate association between perinatal variables and volumes. While the sample size may limit the generalizability of our results, volumetric data in prematurely born young adults suggest similar alterations in the bilateral temporal lobe (Nosarti et al. 2014).

Atypical anatomical covariance is a hallmark of developmental disorders. If the goal of newborn intensive care is to promote typical development for the prematurely born (Bauer and Msall 2010), both critical periods and regions of altered morphometric development need to be explored. Future work should interrogate epigenetic influences contributing to these alterations and develop targeted interventions (Johnson et al. 2009; Thomason et al. 2014).

## Supplementary material

Supplementary Material can be found at <http://www.cercor.oxfordjournals.org/> online.

## Funding

This work was supported by NIH NS27116, NS53865, T32 HD07094, and T32 DA022975.

## Notes

We thank Drs Deborah Hirtz and Walter Allan for scientific expertise; Marjorene Ainley for follow-up coordination; Jill Maller-Kesselman and Victoria Watson for neurodevelopmental testing; and Hedy Sarofin and Terry Hickey for technical assistance. *Conflict of Interest:* None declared.

## References

- Aanes S, Bjuland KJ, Skranes J, Løhaugen GC. 2015. Memory function and hippocampal volumes in preterm born very-low-birth-weight (VLBW) young adults. *Neuroimage*. 105:76–83.
- Alexander-Bloch A, Giedd JN, Bullmore E. 2013. Imaging structural co-variance between human brain regions. *Nat Rev Neurosci*. 14:322–336.
- Alexander-Bloch A, Raznahan A, Bullmore E, Giedd J. 2013. The convergence of maturational change and structural covariance in human cortical networks. *J Neurosci*. 33:2889–2899.
- Back SA, Miller SP. 2014. Brain injury in premature neonates: a primary cerebral dysmaturation disorder? *Ann Neurol*. 75:469–486.
- Ball G, Aljabar P, Zebari S, Tusor N, Arichi T, Merchant N, Robinson EC, Ogundipe E, Rueckert D, Edwards AD, et al. 2014. Rich-club organization of the newborn human brain. *Proc Natl Acad Sci USA*. 111(20):7456–7461.
- Ball G, Boardman JP, Rueckert D, Aljabar P, Arichi T, Merchant N, Gousias IS, Edwards AD, Counsell SJ. 2012. The effect of preterm birth on thalamic and cortical development. *Cereb Cortex*. 22:1016–1024.
- Bassett DS, Bullmore E. 2006. Small-world brain networks. *Neuroscientist*. 12:512–523.
- Bauer SC, Msall ME. 2010. Optimizing neurodevelopmental outcomes after prematurity: lessons in neuroprotection and early intervention. *Minerva Pediatr*. 62:485–497.
- Beck S, Wojdyla D, Say L, Betran AP, Merialdi M, Requejo JH, Rubens C, Menon R, Van Look PF. 2010. The worldwide incidence of preterm birth: a systematic review of maternal mortality and morbidity. *Bull World Health Organ*. 88:31–38.
- Bernhardt BC, Chen Z, He Y, Evans AC, Bernasconi N. 2011. Graph-theoretical analysis reveals disrupted small-world organization of cortical thickness correlation networks in temporal lobe epilepsy. *Cereb Cortex*. 21:2147–2157.
- Bjuland KJ, Rimol LM, Løhaugen GC, Skranes J. 2014. Brain volumes and cognitive function in very-low-birth-weight (VLBW) young adults. *Eur J Paediatr Neurol*. 18:578–590.
- Boardman JP, Counsell SJ, Rueckert D, Kapellou O, Bhatia KK, Aljabar P, Hajnal J, Allsop JM, Rutherford MA, Edwards AD. 2006. Abnormal deep grey matter development following preterm birth detected using deformation-based morphometry. *Neuroimage*. 32:70–78.
- Bullmore E, Sporns O. 2009. Complex brain networks: graph theoretical analysis of structural and functional systems. *Nat Rev Neurosci*. 10:186–198.
- Chen ZJ, He Y, Rosa-Neto P, Gong G, Evans AC. 2011. Age-related alterations in the modular organization of structural cortical network by using cortical thickness from MRI. *Neuroimage*. 56:235–245.
- Constable RT, Vohr BR, Scheinost D, Benjamin JR, Fulbright RK, Lacadie C, Schneider KC, Katz KH, Zhang H, Papademetris X, et al. 2013. A left cerebellar pathway mediates language in prematurely-born young adults. *Neuroimage*. 64:371–378.
- Evans AC. 2013. Networks of anatomical covariance. *Neuroimage*. 80:489–504.
- Foster-Cohen SH, Friesen MD, Champion PR, Woodward LJ. 2010. High prevalence/low severity language delay in preschool children born very preterm. *J Dev Behav Pediatr*. 31:658–667.
- Friederici AD. 2009. Pathways to language: fiber tracts in the human brain. *Trends Cogn Sci*. 13:175–181.
- Garrison KA, Scheinost D, Finn ES, Shen X, Constable RT. 2015. The (in)stability of functional brain network measures across thresholds. *Neuroimage*. 118:651–661.
- Giménez M, Junqué C, Narberhaus A, Bargalló N, Botet F, Mercader JM. 2006. White matter volume and concentration reductions in adolescents with history of very preterm birth: a voxel-based morphometry study. *Neuroimage*. 32:1485–1498.
- Hack M. 2009. Adult outcomes of preterm children. *J Dev Behav Pediatr*. 30:460–470.
- He Y, Chen Z, Evans A. 2008. Structural insights into aberrant topological patterns of large-scale cortical networks in Alzheimer's disease. *J Neurosci*. 28:4756–4766.



- Hille ET, Weisglas-Kuperus N, van Goudoever JB, Jacobusse GW, Ens-Dokkum MH, de Groot L, Wit JM, Geven WB, Kok JH, de Kleine MJ, et al. 2007. Functional outcomes and participation in young adulthood for very preterm and very low birth weight infants: the Dutch Project on Preterm and Small for Gestational Age Infants at 19 years of age. *Pediatrics*. 120:e587–e595.
- Hua X, Leow AD, Parikshak N, Lee S, Chiang MC, Toga AW, Jack CR, Weiner MW, Thompson PM, Initiative AsDN. 2008. Tensor-based morphometry as a neuroimaging biomarker for Alzheimer's disease: an MRI study of 676 AD, MCI, and normal subjects. *Neuroimage*. 43:458–469.
- Inder TE, Huppi PS, Warfield S, Kikinis R, Zientara GP, Barnes PD, Jolesz F, Volpe JJ. 1999. Periventricular white matter injury in the premature infant is followed by reduced cerebral cortical gray matter volume at term. *Ann Neurol*. 46:755–760.
- Johnson MB, Kawasawa YI, Mason CE, Krsnik Z, Coppola G, Bogdanovic D, Geschwind DH, Mane SM, State MW, Sestan N. 2009. Functional and evolutionary insights into human brain development through global transcriptome analysis. *Neuron*. 62:494–509.
- Joshi A, Scheinost D, Okuda H, Belhachemi D, Murphy I, Staib LH, Papademetris X. 2011. Unified framework for development, deployment and robust testing of neuroimaging algorithms. *Neuroinformatics*. 9:69–84.
- Komitova M, Xenos D, Salmaso N, Tran KM, Brand T, Schwartz ML, Ment L, Vaccarino FM. 2013. Hypoxia-induced developmental delays of inhibitory interneurons are reversed by environmental enrichment in the postnatal mouse forebrain. *J Neurosci*. 33:13375–13387.
- Kwon SH, Vasung L, Ment LR, Huppi PS. 2014. The role of neuroimaging in predicting neurodevelopmental outcomes of preterm neonates. *Clin Perinatol*. 41:257–283.
- Lerch JP, Worsley K, Shaw WP, Greenstein DK, Lenroot RK, Giedd J, Evans AC. 2006. Mapping anatomical correlations across cerebral cortex (MACACC) using cortical thickness from MRI. *Neuroimage*. 31:993–1003.
- Mechelli A, Friston KJ, Frackowiak RS, Price CJ. 2005. Structural covariance in the human cortex. *J Neurosci*. 25:8303–8310.
- Ment LR, Ehrenkranz RA, Duncan CC, Scott DT, Taylor KJW, Katz KH, Schneider KC, Makuch RW, Oh W, Vohr B, et al. 1994. Low-dose indomethacin and prevention of intraventricular hemorrhage: a multicenter randomized trial. *Pediatrics*. 93:543–550.
- Mitelman SA, Buchsbaum MS, Brickman AM, Shihabuddin L. 2005. Cortical intercorrelations of frontal area volumes in schizophrenia. *Neuroimage*. 27:753–770.
- Myers EH, Hampson M, Vohr B, Lacadie C, Frost SJ, Pugh KR, Katz KH, Schneider KC, Makuch RW, Constable RT, et al. 2010. Functional connectivity to a right hemisphere language center in prematurely born adolescents. *Neuroimage*. 51:1445–1452.
- Nosarti C, Giouroukou E, Healy E, Rifkin L, Walshe M, Reichenberg A, Chitnis X, Williams SC, Murray RM. 2008. Grey and white matter distribution in very preterm adolescents mediates neurodevelopmental outcome. *Brain*. 131:205–217.
- Nosarti C, Mechelli A, Herrera A, Walshe M, Shergill SS, Murray RM, Rifkin L, Allin MP. 2011. Structural covariance in the cortex of very preterm adolescents: a voxel-based morphometry study. *Hum Brain Mapp*. 32:1615–1625.
- Nosarti C, Nam KW, Walshe M, Murray RM, Cuddy M, Rifkin L, Allin MP. 2014. Preterm birth and structural brain alterations in early adulthood. *Neuroimage Clin*. 6:180–191.
- Papademetris X, Jackowski A, Schultz R, Staib L, Duncan J, Barillot C, Haynor D, Hellier P. 2004. Integrated intensity and point-feature nonrigid registration. In: Barillot C, Haynor DR, Hellier P, editors. *Medical image computing and computer-assisted intervention—MICCAI 2004*. Berlin/Heidelberg: Springer. p. 763–770.
- Peterson BS, Anderson AW, Ehrenkranz R, Staib LH, Tageldin M, Colson E, Gore JC, Duncan CC, Makuch R, Ment LR. 2003. Regional brain volumes and their later neurodevelopmental correlates in term and preterm infants. *Pediatrics*. 111:939–948.
- Peterson BS, Vohr B, Staib LH, Cannistraci CJ, Dolberg A, Schneider KC, Katz KH, Westerveld M, Sparrow S, Anderson AW, et al. 2000. Regional brain volume abnormalities and long-term cognitive outcome in preterm infants. *JAMA*. 284:1939–1947.
- Pritchard VE, Bora S, Austin NC, Levin KJ, Woodward LJ. 2014. Identifying very preterm children at educational risk using a school readiness framework. *Pediatrics*. 134:e825–e832.
- Raz N, Lindenberger U, Rodrigue KM, Kennedy KM, Head D, Williamson A, Dahle C, Gerstorf D, Acker JD. 2005. Regional brain changes in aging healthy adults: general trends, individual differences and modifiers. *Cereb Cortex*. 15:1676–1689.
- Raznahan A, Shaw P, Lalonde F, Stockman M, Wallace GL, Greenstein D, Clasen L, Gogtay N, Giedd JN. 2011. How does your cortex grow? *J Neurosci*. 31:7174–7177.
- Rubinov M, Sporns O. 2010. Complex network measures of brain connectivity: uses and interpretations. *Neuroimage*. 52:1059–1069.
- Rueckert D, Sonoda LI, Hayes C, Hill DL, Leach MO, Hawkes DJ. 1999. Nonrigid registration using free-form deformations: application to breast MR images. *IEEE Trans Med Imaging*. 18:712–721.
- Saigal S, Doyle LW. 2008. An overview of mortality and sequelae of preterm birth from infancy to adulthood. *Lancet*. 371:261–269.
- Saygin ZM, Norton ES, Osher DE, Beach SD, Cyr AB, Ozernov-Palchik O, Yendiki A, Fischl B, Gaab N, Gabrieli JD. 2013. Tracking the roots of reading ability: white matter volume and integrity correlate with phonological awareness in prereading and early-reading kindergarten children. *J Neurosci*. 33:13251–13258.
- Scheinost D, Benjamin J, Lacadie CM, Vohr B, Schneider KC, Ment LR, Papademetris X, Constable RT. 2012. The intrinsic connectivity distribution: a novel contrast measure reflecting voxel level functional connectivity. *Neuroimage*. 62(3):1510–1519.
- Scheinost D, Kwon SH, Shen X, Lacadie C, Schneider KC, Dai F, Ment LR, Constable RT. Forthcoming 2015a. Preterm birth alters neonatal, functional rich club organization. *J Brain Struct Funct*. doi:10.1007/s00429-015-1096-6.
- Scheinost D, Lacadie C, Vohr BR, Schneider KC, Papademetris X, Constable RT, Ment LR. 2015b. Cerebral lateralization is protective in the very prematurely born. *Cereb Cortex*. 25(7):1858–1866.
- Smith SM. 2002. Fast robust automated brain extraction. *Hum Brain Mapp*. 17:143–155.
- Smyser CD, Snyder AZ, Shimony JS, Mitra A, Inder TE, Neil JJ. 2016. Resting-state network complexity and magnitude are reduced in prematurely born infants. *Cereb Cortex*. 26:322–333.
- Staib LH, Jackowski M, Papademetris X. 2006. Brain shape characterization from deformation. *Proc IEEE Int Symp Biomed Imaging*. 3:1140–1143.
- Studholme C, Hill DLG, Hawkes DJ. 1999. An overlap invariant entropy measure of 3D medical image alignment. *Pattern Recognition*. 32:71–86.
- Thomason ME, Brown JA, Dassanayake MT, Shastri R, Marusak HA, Hernandez-Andrade E, Yeo L, Mody S,

- Berman S, Hassan SS, et al. 2014. Intrinsic functional brain architecture derived from graph theoretical analysis in the human fetus. *PLoS ONE*. 9:e94423.
- Thomason ME, Dassanayake MT, Shen S, Katkuri Y, Alexis M, Anderson AL, Yeo L, Mody S, Hernandez-Andrade E, Hassan SS, et al. 2013. Cross-hemispheric functional connectivity in the human fetal brain. *Sci Transl Med*. 5:173ra124.
- Vohr BR, Allan W, Katz KH, Schneider K, Tucker R, Ment LR. 2014. Adolescents born prematurely with isolated grade 2 haemorrhage in the early 1990s face increased risks of learning challenges. *Acta Paediatr*. 103:1066–1071.
- Volpe JJ. 2009. Brain injury in premature infants: a complex amalgam of destructive and developmental disturbances. *Lancet Neurol*. 8:110–124.
- Wilke M, Hauser TK, Krägeloh-Mann I, Lidzba K. 2014. Specific impairment of functional connectivity between language regions in former early preterms. *Hum Brain Mapp*. 35:3372–3384.
- Zielinski BA, Anderson JS, Froehlich AL, Prigge MB, Nielsen JA, Cooperrider JR, Cariello AN, Fletcher PT, Alexander AL, Lange N, et al. 2012. scMRI reveals large-scale brain network abnormalities in autism. *PLoS ONE*. 7:e49172.
- Zielinski BA, Gennatas ED, Zhou J, Seeley WW. 2010. Network-level structural covariance in the developing brain. *Proc Natl Acad Sci USA*. 107:18191–18196.
- Zielinski BA, Prigge MB, Nielsen JA, Froehlich AL, Abildskov TJ, Anderson JS, Fletcher PT, Zygmunt KM, Travers BG, Lange N, et al. 2014. Longitudinal changes in cortical thickness in autism and typical development. *Brain*. 137:1799–1812.